


Encapsulation of CNT Films on Silicon Wafer by DLC Synthesized by PECVD for Application as a Thermal Interface Material



Krishna Ankit , T. Gecil Evangeline, L. S. Aravinda, N. Sharath Kumar, Mamilla Ravi Sankar, Nagahanumaiah, K. Niranjana Reddy, and N. Balashanmugam

1 Introduction

Sumio Iijima's discovery of CNTs opened up research in innovative materials [1]. CNTs are a boon to several capital goods sectors like microelectronics, nanotechnology, biomedical, etc., as they are known to have excellent physical properties.

CNTs are deposited using various chemical vapour deposition techniques. Plasma-enhanced chemical vapour deposition (PECVD) is one technique to synthesize CNTs at a lower substrate temperature than a conventional chemical vapour deposition (CVD). Based on the source of plasma used, PECVD is categorized into radiofrequency (RF), direct current (DC) and microwave (MW) PECVD [2–4]. CNTs with low amorphous carbon content have been deposited using the RF-PECVD technique with parallel plates. This modification effectively reduces the undesirable damage induced by plasma [5]. The growth of CNTs is promoted by factors like pretreatment of the catalyst, vacuum pressure and substrate temperature. In the absence of

K. Ankit (✉) · L. S. Aravinda · Nagahanumaiah · K. N. Reddy · N. Balashanmugam
Central Manufacturing Technology Institute (CMTI), Tumkur Road, Bangalore 560022, India
e-mail: ankit@cmti.res.in

Nagahanumaiah
e-mail: director@cmti.res.in

K. N. Reddy
e-mail: niranjana@cmti.res.in

T. G. Evangeline
Vellore Institute of Technology, Vellore 600097, India

K. Ankit · N. S. Kumar · M. R. Sankar
IIT Tirupati, Tirupati 517506, India
e-mail: evmrs@iittp.ac.in

a plasma, CNTs require to be synthesised at very high temperatures greater than 1000 °C. The presence of plasma facilitates the synthesis of CNTs [3].

CNTs have favourable thermal conduction properties [6]. Microelectronics comprise thin film coatings of AlN over CNTs to enhance thermal conductivity that may help in thermal dissipation [7]. Ion fluids comprising lowered percentages of MWCNTs in an electrochemical cell has improved the power of a thermochemical cell up to 30% [8]. Authors have demonstrated a nine times manifold decrease in thermal resistance when MWCNTs had their surface modified using pyrenylpropylphosphonic acid [9]. Authors have shown a resultant three times higher Carnot efficiency by using MWCNTs. This required the improvement of the cell's Carnot efficiency [10]. Covalent bond-based organic molecules improved adhesion of CNTs with the interfaces and has decreased thermal resistivity by six orders [11]. Some research groups have used photo acoustic technique for calculating total thermal resistance of the system for various CNT matrices [12].

Diamond-like carbon (DLC) is amorphous carbon [13] in its form of metastability and has a high number of sp^3 bonds. DLC can have up to 70% of sp^3 content [14]. The toughness of DLC is improved by incorporating CNTs over DLC which can be used in practical application for imparting hardness [15].

Depositing DLC over CNTs enhances the field emission properties by improving current density and field threshold forming a potential material in the fabrication of field emission devices [16, 17]. DLC deposited over CNTs was reported as the best candidates for field emission applications since they possess combined properties of both CNTs and DLC contributing to its long lifetime, stability and performance [18].

A lot of current global research is focused on usage of CNTs as a thermal interface material (TIM). CNTs offer a poor reliability at 200 μm height with thin film Cu deposited on the former imparting a mismatch in coefficient of thermal expansion [19]. CNTs are also known degrade faster although they have excellent thermal conductivities [20]. CNTs mixed with epoxy offer about 12.2 W/mK of thermal conductivity [21]. High performance vertically aligned CNTs (VACNT) offer potential as a TIM and many companies are trying to incorporate it as heat sinks [22]. Cu foil on plasma modified VACNT offered promise as thermal interface material [23]. TiN, SiO_2 , Ni and Ti have also been deposited on nearly VACNTs and thermal conductivities up to 20 W/mK have been achieved experimentally [24, 25].

It is known that DLC has good thermal conductivity. The current research focuses on the development of DLC/CNT composite by depositing a thin film of DLC over PECVD-based synthesized CNTs for a different flow rate of acetylene. These nanocomposites are evaluated using characterization tools like scanning electron (SEM), transmission electron microscope (TEM), raman spectroscopy, and nanoindentation.

This research aims at development of CNT based DLC nano sandwich which not only enhances the adhesion of CNTs, but also offers a stable thermal interface material. As they are carbon-carbon nanocomposite, thermal mismatch is also avoided as mentioned in prior literature. This method is easily scalable on a wafer and hence can be used directly while fabricating devices in semiconductor fabs. This approach is being taken up as it seems to be one of the practical and industrially viable options

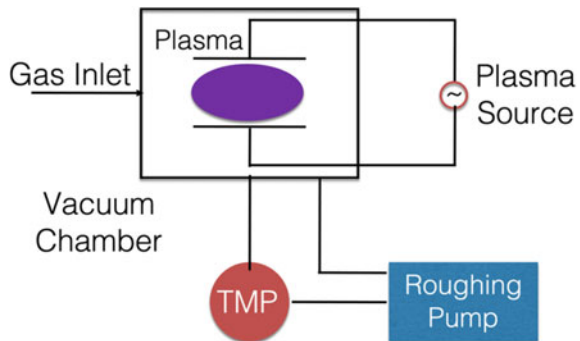
of developing efficient thermal interface materials for electronics and semiconductor applications. DLC of about 500 nm was deposited with flow rates of 300 and 100 sccm to encapsulate CNTs. The method for encapsulation of CNTs has been given in [25].

2 Experimental Details

2.1 Synthesis of CNTs

Silicon substrates of 10 mm^2 are cleaned in mild soap solution to separate impurities and then rinsed again in triple distilled water to eliminate alkali remnants of the soap solution. The wafers are rinsed in isopropyl alcohol which is subjected to a 10 min ultrasonication. The substrates undergo re-rinsing using distilled water to eliminate the alcohol traces. They are later dried in inert argon atmosphere. nickel (Ni) is sputtered using a DC magnetron on the Si substrate and acts as a catalyst for the growth of CNTs. The thickness of Ni is maintained at 5 nm using a calibrated quartz film thickness monitor. The thin layer of nickel anneals in the presence of hydrogen plasma with a flow rate of 200 sccm. The synthesis of CNTs succeeds in the nucleation process of Ni using a radiofrequency plasma-enhanced chemical vapour Deposition (RF-PECVD) (Roth & Rau, Model: HBS-500) system. The radiofrequency is set to 13.56 MHz on the system which is a typical IEEE standard. The ratio of carbon precursor to dilution gas is maintained at 1:8 during the deposition. Vertically aligned CNTs are synthesized for an $\text{C}_2\text{H}_2 / \text{H}_2$ flow rate of 25/200 sccm for a deposition time of 30 min at 600°C (Fig. 1).

Fig. 1 Schematic of the PECVD used for the experimentation



2.2 Deposition of DLC Thin Films

Diamond-like carbon is synthesized on CNT samples using the PECVD technique at 1.17×10^{-3} mbar for the C_2H_2 flow rates of 100 sccm and 300 sccm. A temperature of $350^\circ C$ is maintained for the deposition of a 500 nm thin film of DLC over the CNT sample. The growth rate of DLCs has already been established and measurement techniques have been calibrated as stated in our previous experimentations [26–30].

Method of measurement of DLC. As mentioned above, in our previous experiments [26–30], the procedure was established by using time based deposition for each parameter calibrated for thickness with a spectroscopic ellipsometer (J A Woolam) using a specially developed B-Spline model which has undergone inter laboratory comparison with various other techniques at University of Chemnitz, Germany. Also, the thickness has been calibrated using the in-house surface profiler (Ametek Taly-surf) for step height measurement which has a resolution of 1 nm and is accredited by NABL. A non-contact optical profiler (Veeco NT9100) with a resolution of 0.1 nm has also been used to measure the step height for deposition based on time. These experiments have undergone hundreds of repeatability experiments to measure the deposition. The rate of deposition required to deposit DLC is noted, and 500 nm is deposited in the system. A similar comparative based methodology is also used in our previous work [24, 25].

2.3 Characterization

The synthesized 2D-nanocomposites are characterized using SEM, TEM, Raman and nano indentation. A Neon-40 Crossbeam (Carl Zeiss), FESEM was used to observe the surface morphology of the deposited 2D material. The crystal nature of the DLC/CNT composite is investigated using the Titan G2 60–300 transmission electron microscope (TEM). Raman spectroscopy (SEKI Technotron Corp, STR-300) was used to study the molecular fingerprint and determine the sp^3 and sp^2 content. Ansys software is used to model the thermal simulations.

3 Results and Discussion

3.1 Electron Microscopy

Figure 2 comprises of an SEM image of CNTs having a diameter ranging from 30 to 50 nm. Here 3.a. and 3.b. depict DLC synthesized on CNTs at a temperature of $350^\circ C$ for different C_2H_2 flow rates of 100 and 300 sccm. The high-resolution SEM image magnified up to 100Kx reveals the nature of 500 nm thick DLC layer deposited over CNTs thereby forming clusters of DLC layer on top of CNTs. A similar morphology

is observed in DLC deposited over CNTs at a C_2H_2 flow rate of 300 sccm. Hence, for different flow rates, the morphology observed is similar and shows no much variation. However, for the same contrast used for both the imaging, we can notice that there is a dense core region at the centre for the 300 sccm deposition of DLC and that is reflected in the z-contrast of SEM imaging (Fig. 3).

Figure 4a shows the high-resolution TEM image of DLC coated over CNTs where CNTs are identified by the presence of walls. The SAED pattern in Fig. 4b reveals the presence of both DLC and CNTs which are amorphous. The spots indicate that there is a good amount of crystalline DLC similar to cubic zirconia [29, 31].

Similar results can be observed for DLC deposited over CNTs at a C_2H_2 flow rate of 300 sccm. Figure 5a elucidates the high-resolution TEM image where CNTs are marked by the presence of multiple walls. Figure 5b shows the SAED pattern indicating the presence of both DLC and CNTs which are amorphous. The spots

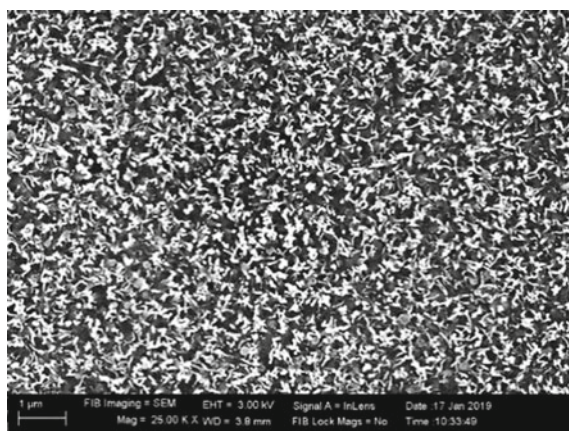


Fig. 2 SEM image of CNTs synthesized for deposition of DLC films

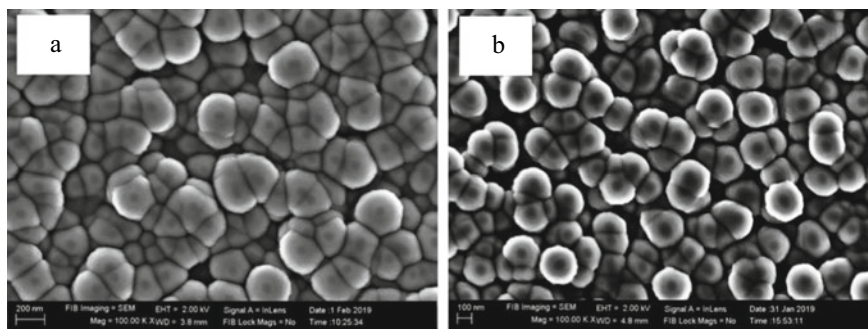


Fig. 3 a DLC coated over CNTs at 100 sccm at 350 °C b DLC coated over CNTs at 300 sccm at 350 °C

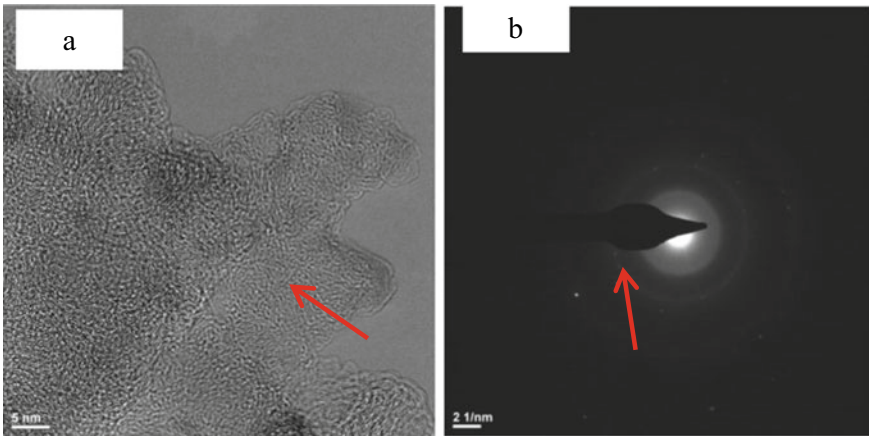


Fig. 4 **a** High-resolution TEM image of DLC coated over CNTs at 100 sccm **b** SAED of DLC coated over CNTs

represent crystalline DLC that exhibits structure similar to cubic zirconia [29, 31]. Region 1 in Fig. 5a shows the crystalline nickel from which CNTs have grown indicating the tip growth mechanism of CNT [32, 33].

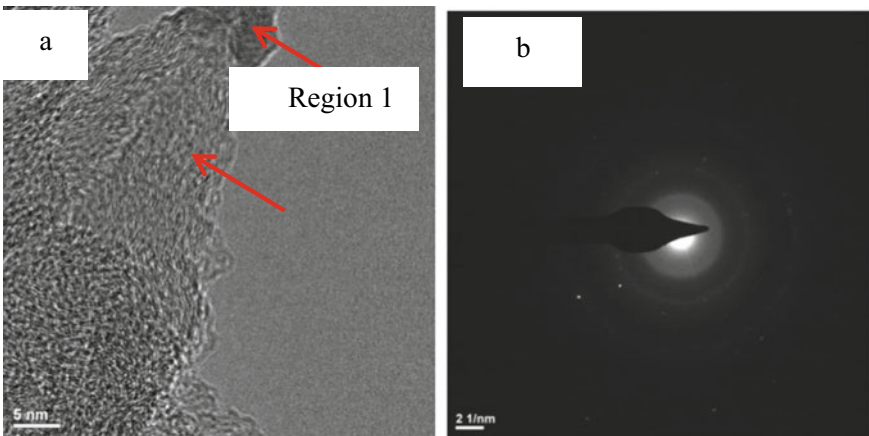
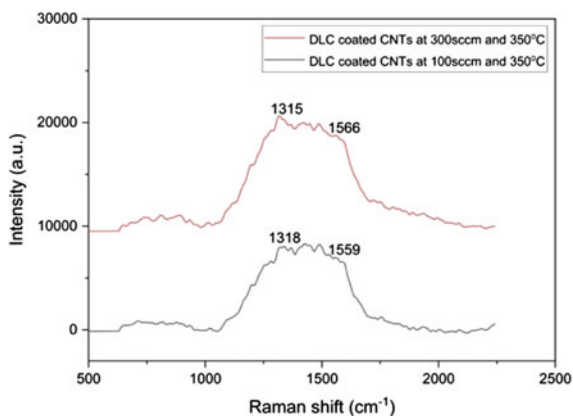


Fig. 5 **a** High-resolution TEM image of DLC coated over CNTs at 300 sccm **b** SAED of DLC coated over CNTs

3.2 Raman Spectroscopy

Carbon films exhibit similar features in their Raman spectra, hence both DLC and CNTs possess common features in the spectrum. DLC is a mixture of amorphous carbon that consists of both sp^3 and sp^2 hybridizations [34]. Figure 6 represents the Raman spectra of DLC/CNT composite for DLC deposition at 350°C for C_2H_2 flow rate at 100 sccm and 300 sccm. DLC/CNT for C_2H_2 flow rate at 100 sccm exhibiting peaks at positions 1318 cm^{-1} and 1559 cm^{-1} corresponding to D peak and G peak, respectively. DLC has an average G peak position ranging from 1581 cm^{-1} to 1600 cm^{-1} which is due to phonon confinement in graphitic domains. In this case, a decrease in G peak shift at 1559 cm^{-1} is observed owing to weaker sp^2 bonds which weaken vibrational modes [35]. Also, the G peak caters to the MWCNTs graphite frequency corresponding to the tangential vibration of carbon atoms [36]. A rise in D peak at position 1318 cm^{-1} corresponds to sp^3 hybridization due to the amorphous nature of DLC deposited over CNTs [16]. In the case of DLC deposited at 300 sccm and for a temperature of 350°C , the Raman spectra show the same characteristics features as that of DLC deposited at 100 sccm. However, it may be noted that for C_2H_2 flowrates of 100 sccm and 300 sccm, the synthesized DLC has a G peak at 1559 cm^{-1} and 1566 cm^{-1} which is close to the a-t:C type of DLC [37]. Although G peak arising at 1515 cm^{-1} corresponds to a-C: H type of DLC [37], it can be safely assumed that the crystalline graphitic content is higher in the current DLC subjected to study and closer to a-t:C DLC. It may also be noted that most of the vibrational signatures arising from the 2D material will be from DLC as it is 500 nm thick.

Fig. 6 Raman spectra of DLC coated over CNTs for C_2H_2 flow rate at 100 sccm and 300 sccm



3.3 Simulation of Heat Transfer

Computer simulations are cost effective methods to study and analyse the thermal properties of the nano sandwich in contention. Simulations are cost-effective to estimate rough thermal conductivities [38]. CNTs are proposed to be advanced material for thermal interfacing in the electronic industry [39]. Experimentally, thermoreflectance methods have been used to measure the thermal conductivity for MWCNTs and have been found to be about 13–17 W/m K [38].

Thermal flux and thermal distribution are analysed and predicted using Ansys software. The following are assumed (1) material is in steady state, (2) heat dissipates from the silicon side to DLC, (3) CNTs are vertically aligned, and (4) Homogeneity in material.

Model of the Si/CNT/DLC 2D nanomaterial was created using solidworks. Although the actual details of the composite are comprised of a Si substrate of 10 mm × 10 mm having a thickness of about 820 μm, CNTs having a length of about 800 nm.

Following are the assumptions taken in solidworks to model: (1) Substrate area: 10 mm² (2) thickness: 825 μm (3) CNT diameter: 100 nm (5) CNT height: 800 nm (6) DLC thickness: 500 nm. Although the diameter of CNT was 40 nm when measured using an SEM, the least diameter of the CNT was 100 nm when modelled using solidworks due to its limitation in modelling very low dimensional features. It can be noted that the results would be slightly coarser, however does not impede any inferences. The thermal analysis of the material considered at steady state was simulated using Ansys software. The boundary conditions fixed for the simulation were the temperature of base substrate Si area was fixed at 80 °C and CNT/DLC thin film matrix was maintained as 26 °C (sink temperature) which is roughly the average room temperature in India. Typically, semiconductors are interlocked to shut down by 80 °C. Hence, this upper cut off temperature is selected. Figure 7. shows the boundary conditions used for the simulation of the 2D-2D nanocomposite material.

R_M is the total resistance of the material, i.e. DLC. R_{CNT} is the total resistance of the CNT, and R_{Si} is the resistance of Silicon wafer.

Thermal resistance is the heat property of a material by which it resists the heat flow. This can be simplified by an equivalent resistance of individual material

$$Re_y = \frac{l_y}{A_y \lambda_y} \quad (1)$$

where

y = Numerical designation to each of the material in contention, i.e. Si, CNT and DLC.

Re = Total resistance of the material, K/W.

l = Length of respective materials, m

λ = Thermal conductivities of the materials, W/mK.

A = Area of the materials, m².

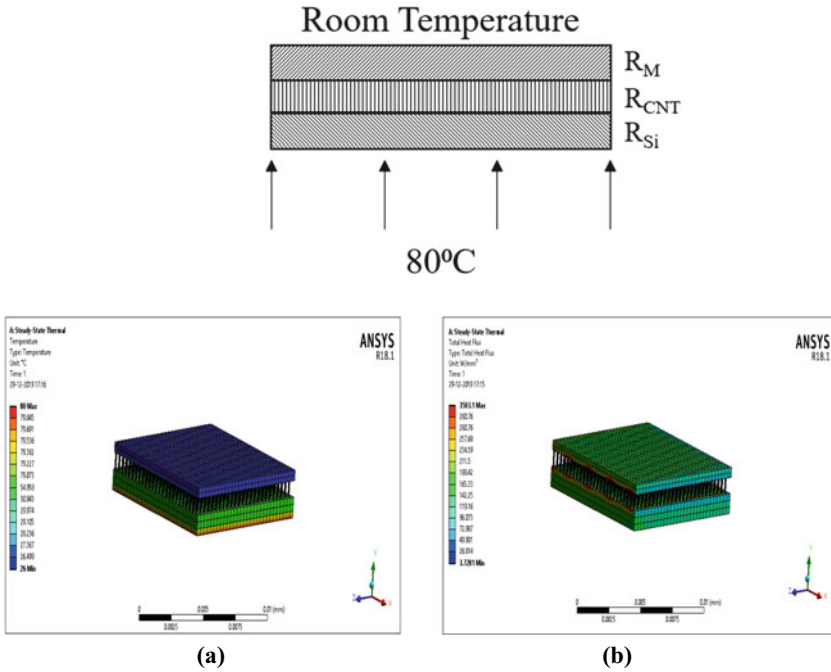


Fig. 7 Modelling of 2D nano composite for thermal simulation **a** Thermal distribution in the matrix **b** thermal flux in the Si/CNT/DLC matrix

Equivalent resistance of CNTs are given by (considered to be in parallel as they are multi-walled vertically aligned):

$$\frac{1}{Re_2} = \sum_{i=1}^n \frac{1}{Re_i} \tag{2}$$

CNT Area:

$$A_{CNT} = \pi dt \tag{3}$$

From the Raman results obtained above, the DLC coating is similar to a:t-C [37]. Hence, the approximate thermal conductivity of the DLC coating considered for calculating the equivalent resistance is 2.2 W/mK at room temperature [39, 40].

The equivalent resistance of the nanocomposite when in series is given by

$$Re_q = Re_1 + Re_2 + Re_3 \tag{4}$$

where

Re_q = Equivalent thermal resistance of the material matrix, K/W.

$t = 0.34$ nm, one carbon atom thickness.

$d =$ CNT Dia, m

$n =$ total CNTs.

Equivalent resistance of the Si/CNT/DLC matrix is determined by the aforementioned mathematical model. This is determined to be 2418.54 K/W. Thermal flux of the material matrix is determined by Ansys simulation using the calculations above which has an equivalent resistance of 73.59 W/mK.

Numerical Simulations. one dimensional heat transfer equation (without considering heat generation) is solved to obtain thermal distribution and total thermal flux of the nano material matrix of the nano sandwich. From simulations, the obtained thermal flux for this matrix is about 245 W/mm² (Fig. 7b).

4 Conclusions

DLC layer of 500 nm thickness was successfully coated over CNTs using the PECVD system at 350 °C for C₂H₂ flow rates of 100 sccm and 300 sccm. There is no substantial change in the thermal flux or dissipation with the change of flowrate, however, 300 sccm comprises larger content of amorphous carbon. SEM image highlights globular structures only encapsulating the top of the CNTs. TEM images show the polycrystalline nature of DLC with CNT in the matrix. The TEM results also give a detailed insight into the phases of the composite through SAED analysis. The Raman spectroscopy of DLC coated CNTs indicate the presence of DLC over CNTs by identifying the corresponding peaks. The Raman spectroscopy peaks provide the presence of DLC and CNTs with Raman Number for D peaks in the range of 1315–1318 cm⁻¹ and G peaks in the range of 1559–1566 cm⁻¹ showing the regime of t-aC:H and a-C:H. From a simulated thermal analysis of the material matrix, it was noted that the thermal flux is 245 W/mm² and the thermal conductivity is 73.59 W/mK.

Acknowledgements The authors thank Mr. Murugan A, Mrs. Sarmistha Dhan, and Mr. Basavaraju, CMTI for assisting in characterization.

References

1. Iijima S (1991) Helical microtubules of graphitic carbon. *Nature* 354:56–58. <https://doi.org/10.1038/354056a0>
2. Meyyappan M, Delzeit L, Cassell A, Hash D (2003) Carbon nanotube growth by PECVD: A review. *Plasma Sources Sci Technol*. <https://doi.org/10.1088/0963-0252/12/2/312>
3. Sato, Hideki & Hata K Growth of carbon nanotubes by plasma-enhanced chemical vapor deposition. *New Diam Front Carbon Technol* 16:163–176
4. Szabó A, Perri C, Csató A et al (2010) Synthesis methods of carbon nanotubes and related materials. *Materials (Basel)* 3:3092–3140. <https://doi.org/10.3390/ma3053092>

5. Yabe Y, Ohtake Y, Ishitobi T, et al (2004) Synthesis of well-aligned carbon nanotubes by radio frequency plasma enhanced CVD method. 13:1292–1295. <https://doi.org/10.1016/j.diamond.2003.11.067>
6. Hone J, Llaguno MC, Biercuk MJ et al (2002) Thermal properties of carbon nanotubes and nanotube-based materials. *Appl Phys A Mater Sci Process* 74:339–343. <https://doi.org/10.1007/s003390201277>
7. Tailleux A, Achour A, Djouadi MA et al (2012) PECVD low temperature synthesis of carbon nanotubes coated with aluminum nitride. *Surf Coatings Technol.* <https://doi.org/10.1016/j.surfcoat.2011.09.048>
8. Salazar PF, Stephens ST, Kazim AH et al (2014) Enhanced thermo-electrochemical power using carbon nanotube additives in ionic liquid redox electrolytes. *J Mater Chem A* 2:20676–20682. <https://doi.org/10.1039/c4ta04749d>
9. Taphouse JH, Smith OL, Marder SR, Cola BA (2014) A pyrenylpropyl phosphonic acid surface modifier for mitigating the thermal resistance of carbon nanotube contacts. *Adv Funct Mater* 24:465–471. <https://doi.org/10.1002/adfm.201301714>
10. Hu R, Cola BA, Haram N et al (2010) Harvesting waste thermal energy using a carbon-nanotube-based thermo-electrochemical cell. *Nano Lett* 10:838–846. <https://doi.org/10.1021/nl903267n>
11. Kaur S, Ravavikar N, Helms BA et al (2014) Enhanced thermal transport at covalently functionalized carbon nanotube array interfaces. *Nat Commun* 5:1–8. <https://doi.org/10.1038/ncomms4082>
12. Cola BA, Xu J, Cheng C, et al (2007) Photoacoustic characterization of carbon nanotube array thermal interfaces. *J Appl Phys* 101. <https://doi.org/10.1063/1.2510998>
13. Robertson J (2002) Diamond-like amorphous carbon. *Mater Sci Eng R Reports* 37:129–281. [https://doi.org/10.1016/S0927-796X\(02\)00005-0](https://doi.org/10.1016/S0927-796X(02)00005-0)
14. Casiraghi C, Ferrari AC, Robertson J (2005) Raman spectroscopy of hydrogenated amorphous carbons. *Phys Rev B-Condens Matter Mater Phys* 72:1–14. <https://doi.org/10.1103/PhysRevB.72.085401>
15. Kinoshita H, Ipeei I, Sakai H, Ohmae N (2007) Synthesis and mechanical properties of carbon nanotube/diamond-like carbon composite films 16:1940–1944. <https://doi.org/10.1016/j.diamond.2007.08.004>
16. Hea F, Lib Z, Lib C, et al Enhanced Field Emission properties of Carbon Nanotubes by coating Diamond-like Carbon layer, 3–5
17. Li Y, Yan X, Wei J et al (2020) Dependence of optimum thickness of Ultrathin Diamond-like carbon coatings over carbon nanotubes on geometric field enhancement factor. *ACS Appl Electron Mater* 2:84–92. <https://doi.org/10.1021/ACSAELM.9B00561>
18. Zanin H, May PW, Hamanaka MHMO, Corat EJ (2013) Field Emission from Hybrid Diamond-like Carbon and Carbon Nanotube Composite Structures
19. Nylander A, Hansson J, Nilsson T et al (2021) Degradation of carbon nanotube array thermal interface materials through thermal aging: Effects of bonding, array height, and catalyst oxidation. *ACS Appl Mater Interfaces* 13:30992–31000. https://doi.org/10.1021/ACSAMI.1C05685/SUPPL_FILE/AMIC05685_SI_001.PDF
20. Nylander A, Hansson J, Samani MK et al (2019) Reliability investigation of a carbon nanotube array thermal interface material. *Energies* 12:1–10. <https://doi.org/10.3390/en12112080>
21. Mohamed M, Omar MN, Ishak MSA et al (2020) Comparison between CNT Thermal Interface Materials with Graphene Thermal Interface Material in Term of Thermal Conductivity. *Mater Sci Forum* 1010:160–165. <https://doi.org/10.4028/WWW.SCIENTIFIC.NET/MSF.1010.160>
22. Ping L, Hou PX, Liu C, Cheng HM (2019) Vertically aligned carbon nanotube arrays as a thermal interface material. *APL Mater* 7:020902. <https://doi.org/10.1063/1.5083868>
23. Zhang Q, Calderon A, Ebbing BR, et al (2020) Thermal properties enhancement of vertically aligned carbon nanotubes-based metal nanocomposites as thermal interface materials. *Front Mater* 7:359. <https://doi.org/10.3389/FMATS.2020.572956/BIBTEX>

24. Krishna A, Gecil Evangeline T, Aravinda LS et al (2020) Synthesis and thermal simulations of novel encapsulated CNT multifunctional thin-film based nanomaterial of SiO₂-CNT and TiN-CNT by PVD and PECVD techniques for thermal applications. *Diam Relat Mater* 109:108029. <https://doi.org/10.1016/J.DIAMOND.2020.108029>
25. Krishna A, Aravinda LS, Murugan A, et al (2021) A study on wafer scalable, industrially applicable CNT based nanocomposites of Al-CNT, Cu-CNT, Ti-CNT, and Ni-CNT as thermal interface materials synthesised by thin film techniques. *Surf Coatings Technol* 127926. <https://doi.org/10.1016/J.SURFCOAT.2021.127926>
26. Varade A, Niranjan Reddy K, Sasen D, et al (2014) Detailed Raman study of DLC coating on Si (100) made by RF-PECVD. In: *Procedia Engineering*
27. Varade A, Krishna A, Reddy KN et al (2014) Diamond-like carbon coating made by RF plasma enhanced chemical vapour deposition for protective antireflective coatings on Germanium. *Procedia Mater Sci* 5:1015–1019. <https://doi.org/10.1016/j.mspro.2014.07.390>
28. Niranjan Reddy K, Varade A, Krishna A, et al (2014) Double side coating of DLC on silicon by RF-PECVD for AR application. In: *Procedia Engineering*
29. Ankit K, Varade A, Reddy N et al (2017) Synthesis of high hardness, low COF diamond-like carbon using RF-PECVD at room temperature and evaluating its structure using electron microscopy. *Diam Relat Mater* 80:108–112. <https://doi.org/10.1016/j.diamond.2017.09.005>
30. Ankit K, Varade A, Niranjan Reddy K et al (2017) Synthesis of high hardness IR optical coating using diamond-like carbon by PECVD at room temperature. *Diam Relat Mater* 78:39–43. <https://doi.org/10.1016/j.diamond.2017.07.008>
31. Kozlov ME, Yase K, Minami N et al (1996) Observation of diamond crystallites in thin films prepared by laser ablation of hard fullerene-based carbon. *J Phys D Appl Phys* 29:929–933. <https://doi.org/10.1088/0022-3727/29/3/062>
32. Sinnott SB, Andrews R, Qian D et al (1999) Model of carbon nanotube growth through chemical vapor deposition. *Chem Phys Lett* 315:25–30. [https://doi.org/10.1016/S0009-2614\(99\)01216-6](https://doi.org/10.1016/S0009-2614(99)01216-6)
33. Danafar F, Fakhru'l-Razi A, Salleh MAM, Biak DRA (2009) Fluidized bed catalytic chemical vapor deposition synthesis of carbon nanotubes-A review. *Chem Eng J* 155:37–48. <https://doi.org/10.1016/j.cej.2009.07.052>
34. Ferrari AC, Robertson J (2004) Raman spectroscopy of amorphous, nanostructured, diamond like carbon, and nanodiamond. *Philos Trans R Soc, A* 362:2477–2512. <https://doi.org/10.1098/rsta.2004.1452>
35. Ferrari AC (2002) Determination of bonding in diamond-like carbon by Raman spectroscopy. *Diam Relat Mater* 11:1053–1061. [https://doi.org/10.1016/S0925-9635\(01\)00730-0](https://doi.org/10.1016/S0925-9635(01)00730-0)
36. Costa S, Borowiak-Palen E, Kruszyńska M et al (2008) Characterization of carbon nanotubes by Raman spectroscopy. *Mater Sci* 26:1–9. <https://doi.org/10.1155/2010/603978>
37. S. Kurtz, Tallant, R. Simpson, K. McCarty, L Bemardez DD and PM (1996) Diamond and Diamond-Like Carbon Films. *Adv Electronic Appl* 46
38. Kumanek B, Janas D (2019) Thermal conductivity of carbon nanotube networks: a review. *J Mater Sci* 54:7397–7427. <https://doi.org/10.1007/s10853-019-03368-0>
39. Panzer MA, Zhang G, Mann D, et al (2008) Thermal properties of metal-coated vertically aligned single-wall nanotube arrays. *J Heat Transfer* 130. <https://doi.org/10.1115/1.2885159>
40. Shamsa M, Liu WL, Balandin AA et al (2006) Thermal conductivity of diamond-like carbon films. *Appl Phys Lett* 89:1–3. <https://doi.org/10.1063/1.2362601>